# An experimental and theoretical investigation into the "worm-hole" effect

Liang Zhao, Jiancang Su, Xibo Zhang, Yafeng Pan, Limin Wang et al.

Citation: J. Appl. Phys. **114**, 063306 (2013); doi: 10.1063/1.4818446
View online: http://dx.doi.org/10.1063/1.4818446
View Table of Contents: http://jap.aip.org/resource/1/JAPIAU/v114/i6
Published by the AIP Publishing LLC.

JOURNAL OF APPLIED PHYSICS **114**, 063306 (2013)

# An experimental and theoretical investigation into the "worm-hole" effect

Liang Zhao,[a] Jiancang Su, Xibo Zhang, Yafeng Pan, Limin Wang, Jinpeng Fang, Xu Sun, Rui Li, Bo Zeng, and Jie Cheng

*Science and Technology on High Power Microwave Laboratory, Northwest Institute of Nuclear Technology, P. O. Box 69 Branch 13, Xi'an, Shannxi 710024, China*

(Received 11 May 2013; accepted 30 July 2013; published online 12 August 2013)

On a nanosecond time scale, solid insulators abnormally fail in bulk rather than on surface, which is termed as the "worm-hole" effect. By using a generator with adjustable output pulse width and dozens of organic glass (PMMA) and polystyrene (PS) samples, experiments to verify this effect are conducted. The results show that under short pulses of 10 ns, all the samples fail due to bulk breakdown, whereas when the pulse width is tuned to a long pulse of 7 $\mu$s, the samples fail as a result of surface flashover. The experimental results are interpreted by analyzing the conditions for the bulk breakdown and the surface flashover. It is found that under short pulses, the flashover threshold would be as high as the bulk breakdown strength ($E_{BD}$) and the flashover time delay ($t_d$) would be longer than the pulse width ($\tau$), both of which make the dielectrics' cumulative breakdown occur easily; whereas under long pulses, that $E_f$ is much lower than $E_{BD}$ and $t_d$ is smaller than $\tau$ is advantageous to the occurrence of the surface flashover. In addition, a general principle on solid insulation design under short pulse condition is proposed based on the experimental results and the theoretical analysis. © *2013 AIP Publishing LLC*.
[http://dx.doi.org/10.1063/1.4818446]

## I. INTRODUCTION

For solid insulation structures, two factors may lead to a catastrophic failure: surface flashover and bulk breakdown. Generally, on a microsecond time scale, the electric field threshold of the surface flashover is lower than that of the bulk breakdown, and insulator failures are mostly caused by surface flashover. Therefore, lots of theories and various methods are developed to enhance the surface flashover threshold on a solid/vacuum[1–8] interface or a solid/liquid[9–13] interface. However, on a nanosecond time, insulators mostly fail due to bulk breakdown rather than surface flashover. Only several literatures reported this abnormal phenomenon, among which, Roth and Chantrenne first observed a bulk breakdown trace in a vacuum insulator ring in the PITHON, which they termed as the "worm-hole" effect due to a worm-hole appearance;[14,15] afterwards, Zhao *et al.* observed the same phenomenon on a coaxial vacuum insulator in the accelerator TPG700.[16] Aside from those results on vacuum/ solid interfaces, there were also bulk breakdown traces on the transformer oil/polymer interfaces, as reported by Wang.[17]

No matter where this effect happens, the time scale for these experiments is nanosecond. Recently, there were also similar traces observed on the insulators used in ultra-wide-band (UWB) generators at Northwest Institute of Nuclear Technology (NINT), the pulse width of which is 600 ps, and the photos of the failed insulators are shown in Fig. 1. From this figure, one can clearly see wormhole-like breakdown traces on the insulator surfaces. In this paper, the term of the "worm-hole" effect is adopted, which is to denote the phenomenon that solid dielectrics are prone to breakdown in bulk rather than on surface on a nanosecond time scale.

According to Fig. 1 as well as the experimental results aforementioned, a "rough" conclusion can be drawn that the bulk breakdown is the main factor leading solid insulation structures to fail on short time scales, rather than the surface flashover. Here, the word "rough" is used, which means that direct comparisons with the same insulator profile under different pulse widths are not reported. In addition, there are little mechanisms for the so-called "worm-hole" effect.

To present a reasonable explanation as well as to derive useful suggestions to avoid the occurrence of the "worm-hole" effect under short pulses, further research is needed. In this paper, an experimental and theoretical investigation for the "worm-hole" effect is presented, which is formulated in five sections. Section II is mainly devoted to experiments, which compare the failure patterns of the same test samples under different pulse widths. Section III is devoted to the theoretical analysis from the perspective of surface flashover threshold and flashover time delay. Based on the theoretical analysis as well as the experimental results, a general principle on solid insulation design is suggested, which is presented in Sec. IV. Section V is for the conclusions in this paper.

## II. EXPERIMENTAL VERIFICATION OF THE WORM-HOLE EFFECT

Two sets of experiments were designed and conducted to compare the failure patterns of dielectrics on different time scales.

### A. Experimental setup

The schematic diagram of the experimental setup is shown in Fig. 2, which mainly comprises of a nanosecond

[a]Author to whom correspondence should be addressed. Electronic mail: zhaoliang0526@163.com. Tel: +86-29-84767621.

 

FIG. 1. Photo of the failed insulators due to bulk breakdown under sub-nanosecond pulses with pulse width of 0.6 ns.

pulse generator, TPG200, a transmission microscope, and a set of control and diagnostic system. The TPG200 is a Tesla-type generator,[18,19] which can produce trapezoidal pulses with a width of 10 ns, a rise and fall time of 3 ns, and a maximum amplitude of 300 kV. By shortening the gas-gap switch of TPG200, quasi sine-wave pulses with a full width at half maximum (FWHM) of 7 $\mu$s can also be produced. The transmission microscope is specially designed with resolution of 0.7 $\mu$m, which can record the images at a rate of 15 frames per second. The control and diagnostic system includes a Rogowski coil, a voltage divider, an oscillograph, and a PC.

A working cycle of the experimental setup is as follows: (1) a trigger signal is launched to the TPG200 via the PC and a microsecond or nanosecond pulse is then generated and imposed on the test sample; (2) the current and voltage waveforms on the sample are recorded on the oscillograph via the Rogowski coil and the voltage divider, and then stored in the PC; (3) the microscopic image of the test sample are also recorded and transmitted to the PC simultaneously via the transmission microscope.

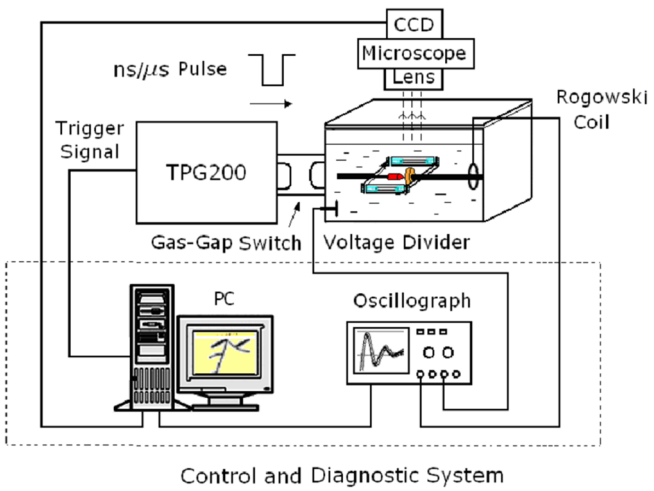


FIG. 2. Schematic diagram of the experimental setup.

## B. Electrodes and test samples

The electrodes are composed of a truncated cone and a plate, both of which are made of copper. The front of the cone is a circle with a diameter of 1 mm, which is parallel to the plate to produce a local quasi-uniform electric field. The plate is cylindrical with a radius of 30 mm. The test samples are made of two types of polymers: PMMA (organic glass, dielectric constant $\varepsilon_r = 3.6$–4, and luminousness 92%) and PS (polystyrene, $\varepsilon_r = 2.4$–2.6, and luminousness 90%). The samples are cubes with a size of $2 \times 2 \times 25$ mm$^3$ (thickness ($d$) $\times$ width $\times$ length), which is to meet both the requirements of observation and insulation.

During the test, the electrodes and a test sample were all immersed in clear transformer oil ($\varepsilon_r = 2.2$–2.3) in order to create a comparable insulation circumstance for the surface and the bulk of the sample. Fig. 3 shows the field distribution on the mid cross-section of a PMMA sample under an applied voltage of 100 kV. Based on this figure, the field distributions along the 'inner line' and the 'surface line' are respectively obtained, as shown in Fig. 4. It is seen that the field distribution along the surface (surface line) and in the bulk (inner line) of the test sample are basically equal to each other, with only an average a relative deviation less than 10%. Therefore, a comparable insulation circumstance is created (Figure 4).

## C. Experimental results

Two sets of experiments are designed and conducted, the first was under a short pulse with width 10 ns, and the second was under a long pulse of 7 $\mu$s. In the short-pulse experiments, the test procedure was as follows: (1) Fixed the applied voltage as $U$; (2) Launched a pulse; (3) Observed the test sample via the microscope, if any bulk breakdown or surface flashover occurred, stopped to shot the pulse; if not, continued to impose the pulse on the test sample until the sample failed. The applied voltage was respectively set as 170 kV, 130 kV, and 100 kV to observe the different failure patterns, and the time interval between each pulse was about 1 s. The test results are listed in Table I, which shows that all the samples failed in bulk breakdown.

By tuning the output pulse width to 7 $\mu$s, the long-pulse experiments were also conducted. Taking into account that

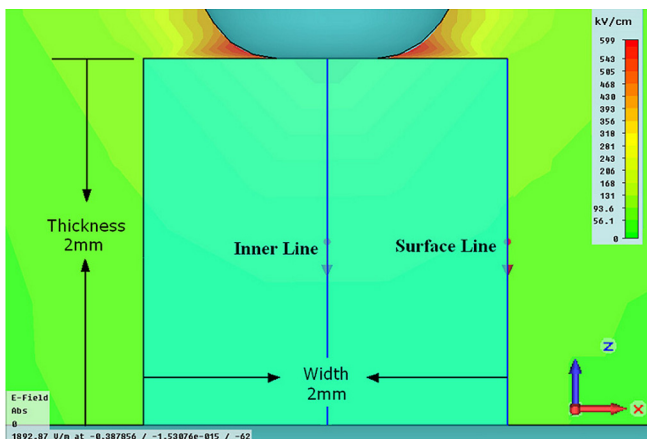


FIG. 3. Electric field distribution on the mid cross-section of the test sample ($y = 0$, $U = 100$ kV)

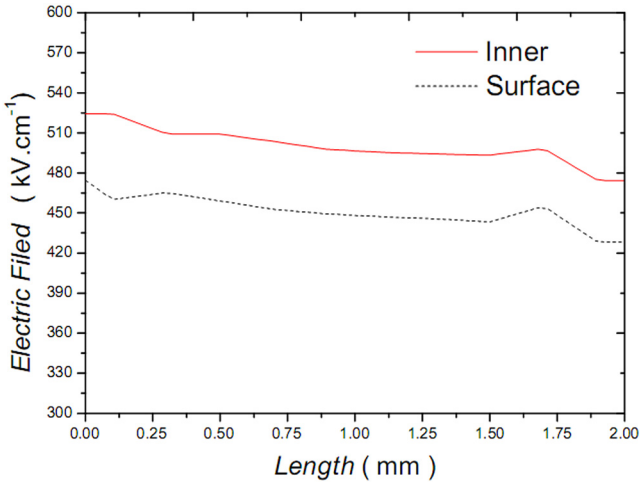


FIG. 4. Electric field distributions along the inner and the surface lines.

the surface flashover would cause the insulation to fail and that a flashover often occurs in one pulse with certain amplitude, we gradually increased the voltage from low to high to find the exact flashover voltage. The experimental results are listed in Table II, which shows that even thought the flashover voltage is different for the two types of polymers, the samples are all failed due to surface flashover. That the flashover voltage of PS is a little higher than that of PMMA is because $\varepsilon_r$ of PS is more closely matched to that of the transformer oil. Similar results under nanosecond pulses in a uniform field can also be seen in Ref. 11.

It is worth mentioning that the number of the test samples for surface flashover in Table II is relatively smaller than that for the bulk breakdown in Table I. This is because lots of researches have been conducted on the surface flashover in oil and it is widely accepted that flashover can cause the insulation to fail under long pulses. It is also worth mentioning that the number of the test sample at low voltage ($U$) in Table I (short pulse) is relative smaller than that at high voltage. This is because the pulse number ($N_L$) is inverse proportional to $U^8$, and a small decrease of $U$ would result in a considerable increase of $N_L$. For example, when $U$ is decreased from 170 kV to 100 kV, $N_L$ is increased from $10^2$ to about $10^4$, the latter of which means a huge work due to one by one count in our experiments.[27] So tests of the samples at low voltage are repeated only by 1–3 times.

To further explore the failure patterns, the typical failure images for each type of samples under different test conditions are compared, as shown in Figs. 5 and 6. From the two

TABLE I. Failure results of PMMA and PS under a short pulse width of 10 ns.

| Sample type | Test voltage/kV | Number of test samples | Failure pattern | Pulse numbers until failure |
|---|---|---|---|---|
| PMMA | 170 | 9 | Bulk | ~300 |
| PMMA | 130 | 2 | Bulk | ~1000 |
| PMMA | 100 | 3 | Bulk | ~10 000 |
| PS | 170 | 2 | Bulk | 328 |
| PS | 130 | 2 | Bulk | ~2000 |
| PS | 100 | 1 | Bulk | 57 453 |

TABLE II. Failure experimental results under a long pulses of 7 $\mu$s.

| Sample type | Failure voltage /kV | Number of test samples | Failure pattern |
|---|---|---|---|
| PMMA | 80 | 2 | Surface |
| PS | 85 | 3 | Surface |

groups of images, it is clearly seen that the bulk breakdown traces are coherent, opaque, and punctured; whereas the surface flashover traces are incoherent, transparent, and random. This is probably due to the place where the failure occurs. For the bulk breakdown, the traces are inside polymers, where the decomposition products such as carbon, short-chain molecules and small gas molecules are confined, which make the traces opaque; whereas for the surface flashover, the traces are on the interfaces, where the products can be easily diffused to the oil, which makes the trace transparent. It is noted that the bulk breakdown traces are totally consistent with the wormhole appearance described in Refs. 14–17.

With the experimental results in Table I, Table II, Figs. 5 and 6, a conclusion can be drawn that solid insulation structures are prone to breakdown in bulk under short pulses, whereas they tend to suffer surface flashover under long pulses.

## III. THEORETICAL ANALYSIS

### A. Failure condition from the perspective of flashover threshold

As aforementioned, on microsecond time scale, the surface flashover threshold ($E_f$) is generally lower than that of the bulk breakdown ($E_{BD}$). However, when the time scale is decreased to a nanosecond time, this conclusion would not hold true. Fig. 7 summarizes the experimental data of $E_f$ dependent on pulse width ($\tau$) on a PMMA/transformer oil interface.[20,21] From this figure, it is seen that in a microsecond pulse width range, $E_f$ is lower than 0.5 MV·cm$^{-1}$; whereas in a pulse width range smaller than 10 ns, $E_f$ is as high as 1 MV·cm$^{-1}$. The latter is close to $E_{BD}$ of polymers under the same pulse width, which can be seen in Ref. 18. Such a high $E_f$ would have influences on the applied field

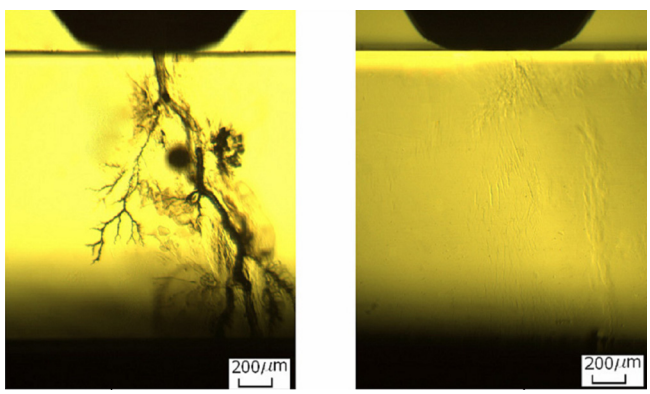


FIG. 5. Comparison for the failure images of PMMA. (a) 10 ns/100 kV/$N = 8733$; (b) 7 $\mu$s/80 kV/$N = 1$, where $N$ represents the pulse number until failure occurs.

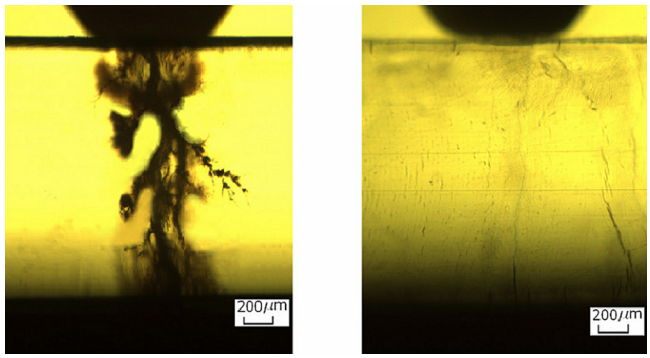


FIG. 6. Comparison for the failure images of PS. (a) 10 ns /170 kV/$N = 328$; (b) 7 $\mu$s/85 kV /$N = 1$.

($E_{op}$), leading to the acceleration of the processes of electron emission and the degradation of polymers.

Taking a 2 mm cylindrical PMMA test sample as an example, the $E_{BD}$(PMMA) $|_{\tau=10\ \mathrm{ns}}$ is 1.6MV·cm$^{-1}$ according to Ref. 18, whereas the $E_f$(PMMA) $|_{\tau=10\ \mathrm{ns}}$ is about 1.2 MV·cm$^{-1}$ from Fig. 6. In practical application, a safe factor ($\beta_s$) which is defined as $E_{BD}/E_{op}$ or $E_f/E_{op}$ is usually set equal to or larger than 2. If $\beta_s = 2$, since $E_{op}$ is smaller than $E_{BD}$, $E_{op}$ $|_{\tau=10\ \mathrm{ns}}$ is set as 0.6 MV·cm$^{-1}$. Under a long pulse condition of 7 $\mu$s, the $E_f$ is about 0.4 MV·cm$^{-1}$. So, the corresponding $E_{op}$ is only 0.2 MV·cm$^{-1}$. According to the famous Fowler-Nordheim formula:[22]

$$j(T) = \frac{1.54\times10^{-6}E^2}{\phi_m}\exp\left(-\frac{6.83\times10^{7}\phi_m^{1.5}}{E}\theta(y)\right)\cdot g(E,\phi_m,T), \tag{1}$$

where $j(T)$ is the current density in A/cm$^2$; $\phi_m$ the work function of the cathode in eV; $\theta(y)$ and $y$ the middle parameters, which are that $\theta(y) = 0.956–1.06y^2$ and $y = 3.8\times10^{-4}\sqrt{E}/\phi_m$; the influence due to the variation of $E_{op}$ on electron emission under different pulse widths can be calculated out. Fig. 8 shows the curves of $j(T)$ dependent on $E_{op}$ for different $\phi_m$. From this figure, it is seen that $j(T)$ for a copper

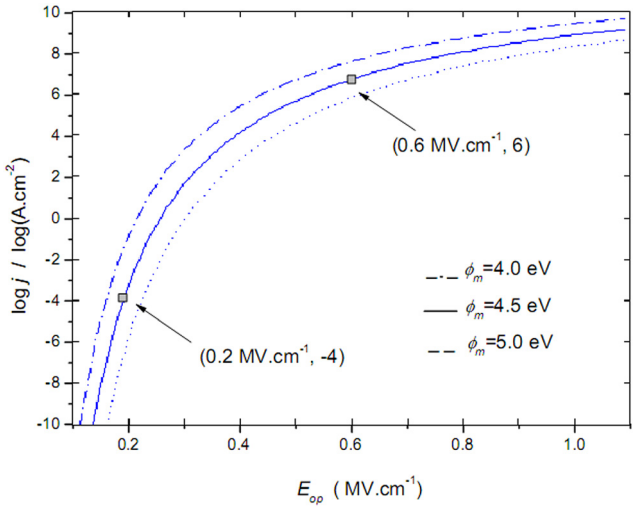


FIG. 8. $j(T)$ versus $E_{op}$ for different work function, where $T$ is set as the room temperature of 300 K.

electrode ($\phi_m = 4.5$ eV) under 10 ns is approximately increased by 10 orders compared with that under 7 $\mu$s. The increase of $j(T)$ accelerates the creation of the 'free radicals', which are the small unpaired molecules in polymers.[23] Fig. 9 shows the density of free radicals ($j_D$) dependent on $E_{op}$ in a wide electric field range.[24] From this figure, it is seen that $j_D$ is increased approximately by 7 orders when the pulse width is tuned from 7 $\mu$s to 10 ns. The cluster of free radicals is advantageous to the formation of the discharge channel in polymers.[25] Once a discharge channel emerges in an insulator, it would grow gradually as the pulse number increases. In this way, a bulk breakdown event may occur and a wormhole trace appears. However, under long pulses, since $E_{op}$ is much lower than that under short pulses, the rate for the creation of free radical is much slower, and the cumulative breakdown is developed with a much slower rate accordingly. When $E_{op}$ is gradually increased, the probability for the surface flashover is increased considerably, which makes the test samples fail in surface flashover.

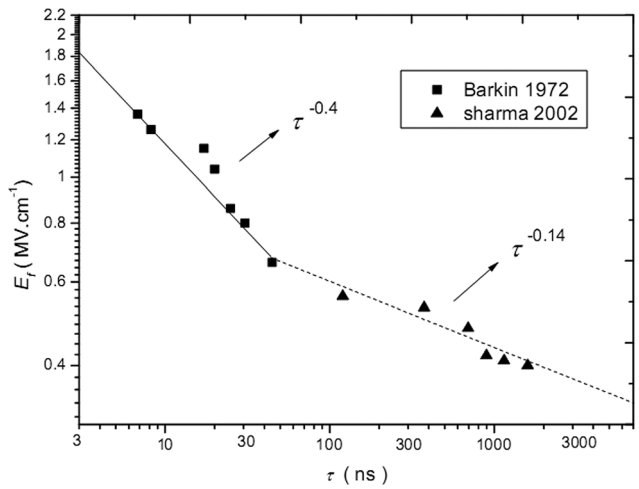


FIG. 7. General tendency of $E_f$ versus $\tau$ on the PMMA/transformer oil interface.

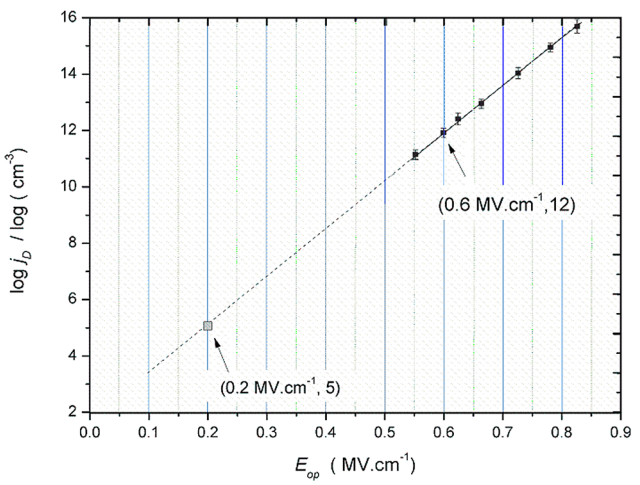


FIG. 9. Density of free radical versus $E_{op}$ in a wide field range. The raw experimental data (solid line) are obtained in Ref. 24.

### B. Failure condition from the perspective of flashover time delay

With the conception of flashover time delay ($t_d$), the different failure patterns for the test samples in short and long pulses can further be explained. $t_d$ is defined the time interval from the time to apply a field to the time when a flashover event occurs. Fig. 10 shows a general tendency of $E_f$ versus $t_d$ for a PMMA/transformer oil interface under nanosecond pulses. From this figure, it is seen that $t_d$ decreases rapidly as $E_f$ increases. In addition, $t_d$ is generally proportional to $E_f^{-1.4}$.

On short time scales, as the pulse width decreases, $t_d$ would be longer than $\tau$, which may make the flashover hard to occur. The underlying reason lies in that the plasma produced by electron multipactor can not cover the distance between cathode and anode timely. However, as the pulse number increases, the discharge channel inside the polymers can increase gradually as aforementioned. Consequently, a bulk breakdown event occurs. Fig. 11 compares the general tendencies of $E_f$ versus $\tau$ and $E_f$ versus $t_d$. From this figure, it is obviously seen that a critical time interval, $t_c$, exists. When the time interval is shorter than $t_c$, $t_d$ would be larger than $\tau$, which may prevent the occurrence of surface flashover, whereas when the time interval is longer than $t_c$, $\tau$ would be longer than $t_d$, which allows the occurrence of surface flashover.

It is considered that the critical time interval is merely a conceptional parameter, which may be affected by many factors, such as dielectric profile, dielectric type, and liquid type, etc., and that the specific value of this parameter is hard to calculate out.

## IV. SUGGESTIONS ON SOLID INSULATION DESIGN

Based on the experimental results and the theoretical analysis, a general principle on solid insulation design under short pulse condition is proposed. On a nanosecond or subnanosecond time scale, since $E_f$ is as large as $E_{BD}$ and the flashover time delay is larger than the pulse width, the focus for solid insulation design should be on how to prevent the dielectrics' inner bulk breakdown, rather than the conventional surface flashover. For a specific insulation structure, if the lifetime, $N_L$, is required to be no smaller than a given value, then by modifying the dielectric thickness, $d$, or the applied voltage, $U$, this requirement can be realized with the following formula:[27]

$$N_L = d^7 \left(\frac{E_1}{U}\right)^8, \tag{2}$$

where $E_1$ is the $E_{BD}$ for a unit dielectric thickness, which represents the dielectric type. The units for a set of $d$, $E_1$ and $U$ are, respectively, mm, kV, and kV·mm$^{-1}$ or cm, MV, and MV·cm$^{-1}$. Still taking a 2 mm PMMA sample as an example, since $E_1(\text{PMMA})|_{d=1\text{mm},\ \tau=10\text{ ns}}=173\text{ kV·mm}^{-1}$, if $N_L$ is required to be larger than $1\times10^4$, then $U$ should be no greater than 100 kV. Similarly, for a PMMA sample to suffer pulse number greater $1\times10^4$, if the sustained voltage is fixed as 200 kV, then the sample should be thicker than 4.4 mm, accordingly.

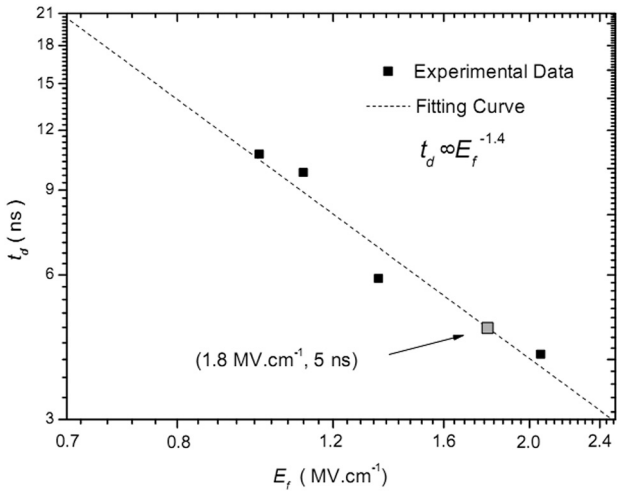


FIG. 10. Fit for the tendency of $t_d$ versus $E_f$ in a log-log coordinate system. The raw experimental data are from Ref. 26.

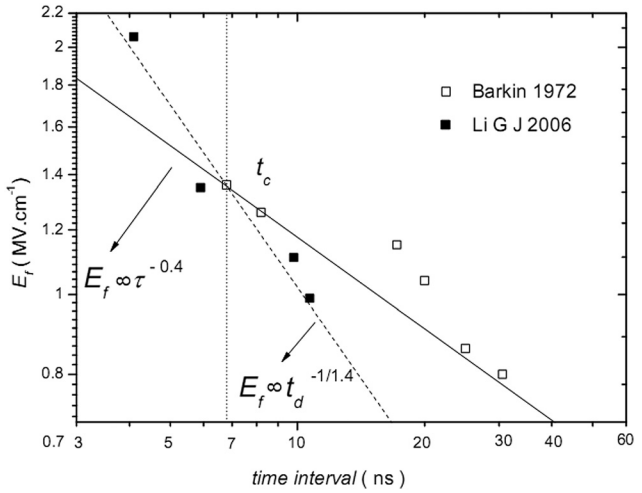


FIG. 11. Comparison of the general tendencies of $E_f$ versus $\tau$ and $E_f$ versus $t_d$ in a log-log coordinated system.

## V. CONCLUSIONS AND REMARKS

In summary, the famous "worm-hole effect" that solid dielectrics are prone to fail due to bulk breakdown on short time scales is experimentally verified by conducting the failure experiments using the same PMMA and PS test samples under pulse widths of 10 ns and 7 $\mu$s, respectively. In addition, by summarizing the tendency of $E_f$ versus $\tau$ on a PMMA/transformer oil interface and by fitting the experimental data of $t_d$ versus $E_f$ in the literatures, it is concluded that on a nanosecond time scale, $E_f$ is as large as $E_{BD}$ and $t_d$ is larger than $\tau$, both of the two which are responsible for the occurrence of the "worm-hole effect."

The theoretical analysis for the "worm-hole effect" is presented only from the perspective of surface flashover threshold and flashover time delay in this paper. As a matter of fact, on a nanosecond scale, the electric field rise-up rate, $\partial E/\partial t$, would be greater than that on a microsecond time scale by three orders for the same applied voltage generally. In addition, the polarization mechanism of polymers on a

nanosecond time scale is different from that on a microsecond time scale.[28] Whether the two differences have influences on the occurrence of the "worm-hole effect" should also be studied in future.

## ACKNOWLEDGMENTS

The author gratefully acknowledges the contributions of Q. Ge and Q. Lin for their help on the experiments.

[1]H. C. Miller, IEEE Trans. Electr. Insul. **24**, 765 (1989).
[2]H. C. Miller, IEEE Trans. Electr. Insul. **28**, 512 (1993).
[3]O. Milton, IEEE Trans. Electr. Insul. **EI-7**, 9 (1972).
[4]C. Chang, J. Y. Fang, Z. Q. Zhang, C. H. Chen, C. X. Tang, and Q. L. Jin, Appl. Phys. Lett. **97**, 141501 (2010).
[5]C. Chang, H. J. Huang, G. Z. Liu, C. H. Chen, Q. Hou, J. Y. Fang, X. X. Zhu, and Y. P. Zhang, J. Appl. Phys. **105**, 123305 (2009).
[6]C. Chang, G. Z. Liu, C. X. Tang, C. H. Chen, H. Shao, and W. H. Huang, Appl. Phys. Lett. **96**, 111502 (2010).
[7]P. Yan, T. Shao, J. Wang, W. Gao, W. Yuan, R. Pan, S. Zhang, and G. Sun, IEEE Trans. Dielectr. Electr. Insul. **14**, 634(2007).
[8]R. A. Anderson and J. P. Brainard, J. Appl. Phys. **51**, 1414 (1980).
[9]M. P. Wilson, M. J. Given, I. V. Timoshkin, S. J. MacGregor, M. A. Sinclair, K. J. Thomas, and J. M. Lehr, IEEE Trans. Plasma Sci. **38**, 2611 (2010).
[10]M. P. Wilson, S. J. MacGregor, M. J. Given, I. V. Timoshkin, M. A. Sinclair, K. J. Thomas, and J. M. Lehr, IEEE Trans. Dielectr. Electr. Insul. **16**, 1028 (2009).
[11]M. P. Wilson, I. V. Timoshkin, M. J. Given, and S. J. MacGregor, IEEE Trans. Dielectr. Electr. Insul. **18**, 1003 (2011).
[12]A. Sharma, S. Acharya, K. V. Nagesh, R. C. Sethi, U. Kumar, and G. R. Nagabhushana, presented at the IEEE 31st International Conference on Plasma Science (2004).
[13]W. L. Huang and Z. X. Cheng, IEEE Trans. Dielectr. Electr. Insul. **17**, 1938 (2010).
[14]S. Chantrenne and P. Sincerny, in *Procedings of the 12th IEEE Inernational Pulsed Power Conference* (Monterey, California, 1999), pp. 1403–1407.
[15]I. S. Roth, P. S. Sincerny, L. Mandelcorn, M. Mendelsohn, D. Smith, T. G. Engel, L. Schlitt, and C. M. Cooke, in *Procedings of the 11th IEEE International Pulsed Power Conference* (IEEE, Baltimore, Md, 1997), pp. 537–542.
[16]L. Zhao, J. C. Peng, Y. F. Pan, X. B. Zhang, and J. C. Su, IEEE Trans. Plasma Sci. **38**, 1369 (2010).
[17]J. Wang, P. Yan, S.-C. Zhang, and G.-S. Sun, presented at the Proceedings of the 15th IEEE International Pulsed Power Conference (2005).
[18]L. Zhao, G. Liu, J. Su, Y. Pan, and X. Zhang, IEEE Trans. Plasma Sci. **39**, 1613 (2011).
[19]L. Zhao, J. C. Su, X. B. Zhang, and Y. F. Pan, IEEE Trans. Dielectr. Electr. Insul. **19**, 1101 (2012).
[20]A. Sharma, K. V. Nagesh, R. C. Sethi, U. Kumarm and G. R. Nagabhushana, presented at the IEEE International Vacuum Electronics Conference (2002).
[21]B. B. Bakin and V. Y. Ushakov, Electronics (Russia) **4**, CTP,76 (1972).
[22]H. Bluhm, *Pulsed Power Systems* (Springer, Karlsruhe Germany, 2006), Chap. 2.
[23]Z. Li, Y. Yin, X. Wang, D. M. Tu, and K. C. Cao, J. Appl. Polym. Sci. **89**, 3416 (2003).
[24]K. C. Kao, *Dielectric Phenomenon in solid* (Elsevier academic press, Amsterdam, 2004), Chap. 8.
[25]H. K. Xie and K. C. Kao, IEEE Trans. Electr. Insul. **EI-20**, 293 (1985).
[26]G. J. Li, "Experimental Study on Dielectric Surface Flashover under Nanosecond Pulse in Transformer Oil," Master of Engineering Graduate (University of the Chinese Academy of Sciences, Beijing, 2006), Chap. 4.
[27]L. Zhao, J. C. Su, X. B. Zhang, Y. F. Pan, L. M. Wang, X. Sun, and R. Li, IEEE Trans. Plasma Sci. **41**, 165 (2013).
[28]L. Zhao, J. C. Su, Y. F. Pan, and X. B. Zhang, Chin. Phys. B **21**(3), 033102 (2012).